

Data-driven cortex segmentation in reconstructed fetal MRI by using structural constraints

Benoît Caldairou, Nicolas Passat, Piotr Habas, Colin Studholme, Mériam Koob, Jean-Louis Dietemann, François Rousseau

▶ **To cite this version:**

Benoît Caldairou, Nicolas Passat, Piotr Habas, Colin Studholme, Mériam Koob, et al.. Data-driven cortex segmentation in reconstructed fetal MRI by using structural constraints. International Conference on Computer Analysis of Images and Patterns (CAIP), 2011, Seville, Spain. pp.503-511, 10.1007/978-3-642-23672-3_61 . hal-01695055

HAL Id: hal-01695055
https://hal.univ-reims.fr/hal-01695055

Submitted on 3 Mar 2018

HAL is a multi-disciplinary open access archive for the deposit and dissemination of scientific research documents, whether they are published or not. The documents may come from teaching and research institutions in France or abroad, or from public or private research centers.

L'archive ouverte pluridisciplinaire **HAL**, est destinée au dépôt et à la diffusion de documents scientifiques de niveau recherche, publiés ou non, émanant des établissements d'enseignement et de recherche français ou étrangers, des laboratoires publics ou privés.

Cortex segmentation in reconstructed fetal MRI by using structural constraints

B. Caldairou*[1], N. Passat[1], P. Habas[2], C. Studholme[2], M. Koob[3], J.-L. Dietemann[3], F. Rousseau[1]

[1]LSIIT, UMR 7005 CNRS-Université de Strasbourg, France
[2]BICG, University of Washington, Seattle, USA
[3]LINC, UMR 7237 CNRS-Université de Strasbourg, France

Abstract. *In utero* fetal MR images are essential for the diagnosis of abnormal brain development and understanding brain structures maturation. Because of particular properties of these images, such as important partial volume effect and tissue intensity overlaps, few automated segmentation methods have been developed so far compared to the numerous ones existing for the adult brain anatomy. In order to address these issues, we propose a two-step atlas-free cortex segmentation technique including anatomical priors and structural constraints. Experiments performed on a set of 6 *in utero* cases (gestational age from 25 to 32 weeks) and validations by comparison to manual segmentations illustrate the necessity of such constraints for fetal brain image segmentation.

Keywords: Cortex, fetal brain, segmentation, topology

1 Introduction

The study of *in utero* developing brain by magnetic resonance imaging (MRI) is motivated by the need of understanding the early brain structure maturation [15, 11]. A prerequisite is the automated labeling of these structures, which has to be robust to noise, fetal motion artifacts, partial volume effects (PVE), and MRI intensity inhomogeneity.

Other studies focused mainly on premature, noenates and young children. Prastawa *et al.* [13] developed an automated segmentation process of the newborn brain, including estimation of the initial parameters through a graph clustering strategy, intensity inhomogeneity correction and a final refinement focusing on the separation of myelinated and non-myelinated white matter regions. White matter delineation from deep grey matter was also a challenge addressed by Murgasova *et al.* [9] for young children with an atlas-based approach. Another method by Xue *et al.* [16], focusing on cortex segmentation and reconstruction through a mislabeled partial volume voxel removal strategy was applied to term and preterm neonates.

* The research leading to these results has received funding from the European Research Council under the European Community's Seventh Framework Programme (FP7/2007-2013 Grant Agreement no. 207667).

A first attempt for fetal brain structures segmentation was a semi-automated algorithm based on a region-growing method by Claude *et al.* [4]. Later on, fully automatic techniques were developed. Bach Cuedra *et al.* [1] introduced separated Bayesian segmentation and Markov random field regularization steps, the latter including anatomical priors. Other methods took advantage of motion-corrected and high resolution 3D volumes, computed through reconstruction techniques from *in utero* MR scans [8, 14]. Habas *et al.* developed an automatic atlas-based segmentation [7], and a method including anatomical constraints in form of a laminar prior [6]. Gholipour *et al.* [5] performed a volumetric study of the brain based on the segmentation of the pericerebral fluid spaces (PFS) (the part of the cerebrospinal fluid (CSF) located around the cortical area) by using level-sets, connected components, and mathematical morphology filters.

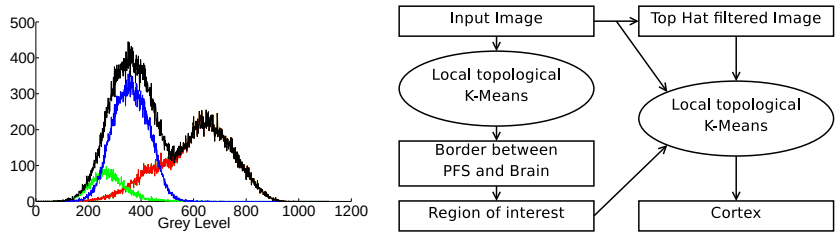
Most of these methods follow an atlas-based approach or specific regularization strategies, including anatomical priors. This illustrates the difficulty to define a data-driven segmentation, because of PVE and important tissue intensity overlaps. Nevertheless, building and using an atlas presents several difficulties such as its registration over the different cases in order to have an accurate segmentation. Moreover, using a specific regularization strategy disconnected from the data illustrates the need of strong structural constraints which can be also used in a data-driven approach.

An atlas-free two-step segmentation is defined. It includes structural constraints based on a topological model [12] in order to deal with PVE, and a morphological filter [10] in order to highlight areas where the cortex will the most likely appear. The first step aims at defining a region of interest including the cortex and the second one aims at segmenting the cortex itself. Experiments are carried out on reconstructed 3D volumes and the probability maps issued from of a non-local fuzzy c-means (NL-FCM) clustering algorithm [3] are used in order to benefit from its robustness to noise.

2 Method

The grey level histogram from fetal MRI (Fig. 1(a)) reveals two peaks corresponding respectively to the brain, including white matter and cortex, and to the CSF. Moreover, an important overlap due to intensity inhomogeneity and partial volume effect is observed. Furthermore, an analysis from a ground truth segmentation reveals that the cortex and white matter peaks are blended into the brain one, meaning that these structures can not be dissociated by classic clustering algorithms based on intensity features. This leads to hazardous classifications such as white matter between CSF and cortex, which is anatomically wrong.

To cope with the previous problems, a two steps segmentation is defined in order to consider these facts (Fig. 1(b)). Both steps rely on a topological k-means described in Section 2.1. Section 2.2 describes the complete segmentation pipeline. The first step aims at separating the intracranial volume into PFS, ventricles and brain. This first segmentation provides a good estimation of the



(a) (b)

Fig. 1. (a) Grey-level histogram from a fetal brain MRI. Black: intracranial volume, green: cortex, red: white matter and deep grey *nuclei*, blue: CSF. (b) Overall diagram of the segmentation process.

border between the PFS and the brain, which is used to define a region of interest including the cortex. Afterward, the second step is performed in order to retrieve the CSF, the white matter and the cortex.

2.1 Topological K-Means

A topological model robust to intensity inhomogeneity, relying on three concentric spheres and introducing geometrical constraints for the segmentation process is defined.

Let us consider an image composed of a set of voxels Ω, each voxel $j \in \Omega$ having a given grey-level $\mathbf{y}_j$. Let us suppose that this image has to be segmented into K (≥ 2) clusters. For each cluster k, let S_k be the set of voxels included into it and ν_k be the centroid of this cluster (which usually corresponds to the mean grey-level value of this class of voxels). Based on these notations, in the k-means approach, the segmentation process of a grey-level image consists of the minimization of an objective function:

$$J_{k\text{-}means} = \sum_{k=0}^{K} \sum_{\mathbf{y}_j \in S_k} \|\mathbf{y}_j - \nu_k\|_2^2.$$

Nevertheless, considering a global centroid (therefore spatially invariant) makes the k-means algorithm sensitive to intensity inhomogeneity occurring in MRI data. In order to tackle this problem without relying on *ad hoc* prior knowledge related to the intensity inhomogeneity, we introduce local intensity centroid values ν_{jk}. These local mean-values are computed in the following way (Fig. 2(a)). An image is divided into several cubical non-overlapping sub-images or regions. Let ν_k^r be the mean value of the kth cluster in an image region r. This region mean value is considered as being located in the center of this region. Let p_r be this position. Afterward, for each considered voxel, a local mean value ν_{jk} is computed by a distance-based interpolation of the nearest region mean-values: $\nu_{jk} = \frac{\sum_r \omega_{jr}\nu_k^r}{\sum_r \omega_{jr}}$, where $\omega_{jr} = 1/d(j,p_r)$ and $d(j,p_r)$ is the Euclidean spatial distance between the voxel j and p_r.

The minimization of the k-means objective function is achieved by a border voxel exchange, with respect to the following topological model. Let N_j be the

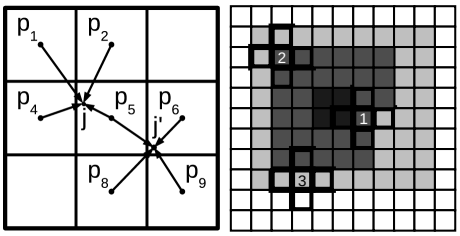


Fig. 2. (a) Intensity inhomogeneity correction. Voxel j mean values depend on mean values from regions 1, 2, 4 and 5 and voxel j' mean values depend on mean values from regions 5, 6, 8 and 9. (b) Topological model. From white to dark grey, labels are 0, 1, 2 and 3, 0 being the background. Voxel 1: not eligible for switching to another label because there are three different labels in its neighborhood and a switch would break the concentric circle model. Voxel 2: eligible to switch to label 1. Voxel 3: not eligible to switch to label 2 because a neighbor is a background label.

neighborhood of voxel j. Let C_{N_j} be the corresponding set of clusters present in N_j. A considered voxel j switches from cluster k to another candidate cluster k' if it meets the following requirements (Fig. 2(b)):

$$\begin{cases} |C_{N_j}| = 2, \\ \forall\ c \in C_{N_j}, c \neq \text{ background}, \\ \|\mathbf{y}_j - \nu_{jk'}\|_2 < \|\mathbf{y}_j - \nu_{jk}\|_2. \end{cases}$$

The first two requirements guarantee the preservation of the structural constraints. They state that a voxel is eligible for switching from one cluster to another if there are exactly two different clusters in its neighborhood, and if neither of these is the background. The third requirement guarantees that a voxel switch decreases the objective function. Our model is different from the notion of simple points used in topology [12], which implies in particular that labels connected components are preserved. Broadly speaking, labels connected components can be broken into several ones or fused as long as the concentric sphere model is respected, which brings a better flexibility to the segmentation process.

In practice, the segmentation is achieved by considering a list of border voxels obtained by a dilation of the current label. Each voxel meeting the third requirement is switched to the considered label. When no switch through the different labels is observed, the centroids are updated and the k-means objective function computed. This process iterates until a local minimum of the objective function is reached.

2.2 Proposed segmentation algorithm

Step 1 - CSF This step is initialized as follows. The intracranial volume, is divided into three concentric spheres representing the PFS, the brain and the ventricles, thanks to an intracranial distance map. Moreover, a two class FCM clustering is performed in order to obtain an accurate initialization of the

centroids. The segmentation is then performed by the topological k-means with the grey-level image as input.

Step 2 - Cortex Due to intensity overlaps between cortex and white matter, additional information is needed in order to achieve the segmentation. Since the fetal cortex is a thin layer between PFS and white matter, a morphological filter is defined in order to highlight image areas where it will most likely appear. Let $I : \Omega \rightarrow V$ be a discrete grey-level image. Let φ_B be the morphological closing of I by a structuring element B. The Top Hat Dark Filter T_d is defined as: $T_d(I) = \varphi_B(I) - I$. In other words, this filter highlights small objects of the image that are removed by the closing, depending on the choice of the structuring element [10].

A region of interest is defined from the border between the PFS and the brain. A band around this border, including CSF and brain is defined thanks to a distance map computed from the PFS segmentation. This band is divided into three sub-bands being the initialization for CSF, cortex and white matter. Moreover, this initialization is corrected by removing any voxel belonging to the ventricles.

The segmentation is performed by using a vector composed by the original image and the top-hat filtered image, instead of the original grey-level values alone, as the input of the topological segmentation presented in Section 2.1. Consequently, each cluster is characterized by a centroid vector composed of its grey-level mean-value and its top-hat-filtered image mean value, allowing a better discrimination of the cortex. During this process, a maximum cortical thickness of 4 millimeters is imposed in order to cope with improbable extensions.

In order to improve the segmentation, one can use probability maps computed from a non local FCM algorithm [3] as a post-processing. This method introduces a regularization based on the non-local framework [2], aiming at correcting artifacts due to noise, by taking advantage of the redundancy present in images. Broadly speaking, a small neighborhood around a voxel, called a patch, may match patches around other voxels within the same scene, selecting the most accurate voxels to perform the regularization. This post-processing step is run on the same border voxel exchange basis than the topological k-means algorithm, unless a voxel may switch if the probability it belongs to the destination label is higher than the current one.

3 Experiments and Results

3.1 Material and experimental settings

Experiments are performed on a set of six patients. Gestational ages (GA) range from 27 to 32 weeks. For each of them, a set of three T2-weighted MR images (axial, coronal and sagittal) are acquired from a 1.5T scanner (Magnetom Avanto, Siemens, Germany Erlangen) using single shot fast spin echo sequences (TR 3190 ms, TE 139-147 ms). Since these images have anisotropic voxel sizes

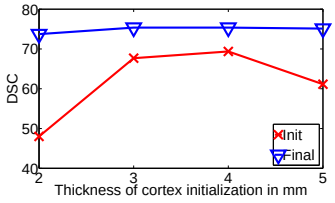


Fig. 3. Average DSC comparison between cortex thickness initialization (red) and final segmentation (blue).

Case (GA)	1 (28)	2 (30)	3 (-)	4 (32)	5 (27)	6 (30)
DSC	72.42	73.03	77.57	74.51	76.60	76.61
DSC with regularization	71.02	71.37	77.76	71.86	75.78	75.23

Table 1. Sensitivity (Sen) and Dice similarity coefficient (DSC) between manual and automated segmentations with and without non-local FCM post-processing.

and may present motion artifacts, a reconstruction process [14] is applied in order to obtain high resolution images.

Reconstructed images have the following dimensions: $256 \times 256 \times 88$ to $256 \times 256 \times 117$ and voxel dimensions are: $0.742 \times 0.742 \times 0.742$ mm. A 3D 6-neighborhood is used to run the topological model. Empirically, a $5 \times 5 \times 5$ structuring element is chosen to perform the Top Hat filter.

For the PFS segmentation, the model is initialized as follows. On the border with the background, a 1 voxel thin layer is set as PFS. Then, the voxels being less than 80% of the maximum intracranial distance are set as brain and the remaining ones are set as ICSF. This guarantees that the ICSF initial cluster will not include any PFS voxels.

Regarding the cortex segmentation, the model was initialized as follows. The first two-millimeters layer is set as CSF, the next 5 as cortex and the last 2 as white matter. These values were chosen according to tissues anatomical characteristics.

Concerning the parameters of the non-local FCM algorithm, the size of the research area is $11 \times 11 \times 11$ and the size of the patches is $3 \times 3 \times 3$. The computation times are about 20 minutes for the extraction of the CSF and 15 minutes for the cortex segmentation.

3.2 Validation

Each reconstructed image has been manually segmented. The validation consists of the computation of the dice similarity coefficient (DSC) between the manual and the automated segmentation of the cortex. Let TP be the amount of true positives (number of detected cortex voxels), FP the amount of false positives (number of voxels incorrectly classified as cortex) and FN the amount of false negatives (number of undetected cortex voxels). The dice coefficient is given by: $DSC = 2 \times TP/(2 \times TP + FN + FP)$.

Table 1 presents Sen and DSC for each case. Both regularized and non-regularized results are presented. Fig. 3 illustrates the algorithm robustness to initialization by setting a 2 to 5 millimeters initial thickness to the cortex.

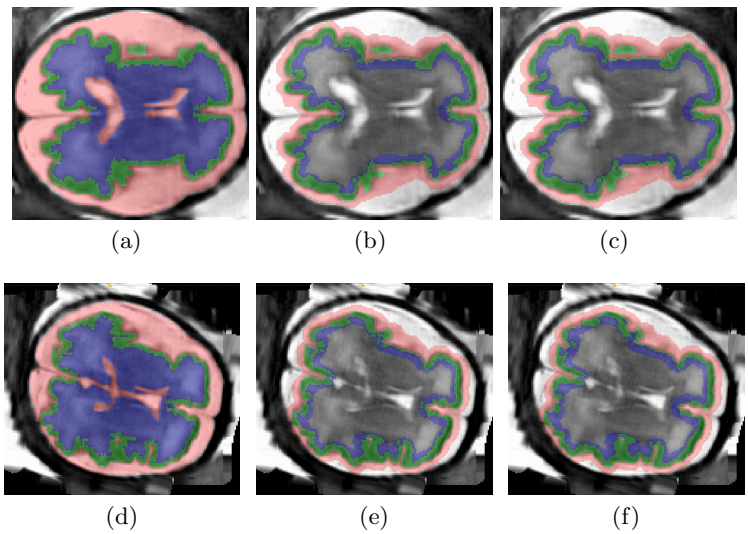


Fig. 4. Cortex extraction. (a,d): ground truth, (b,e): segmentation without non-local FCM regularization, (c,f): segmentation with non-local FCM regularization. Red: CSF, green: cortex, blue: white matter and deep grey *nuclei*.

A visual insight of the segmentation (Fig. 4) underlines the accuracy of the method, even though a slight under-segmentation can be observed in some areas. Moreover, even though regularization accentuates the under-segmentation, it can be observed that it brings a noise correction and smoother borders between the different tissues.

Other studies about fetal brain segmentations highlighted results about the cortex segmentation. Bach Cuedra *et al.* [1] showed *DSC* values around 65 % with a two steps segmentation separating LCR into PFS and ICSF and applying a specific regularization step. Habas *et al.* [7] achieved performance around 82 % with an atlas based approach. Results presented here underline the usefulness of structural constraints for fetal tissue segmentation, if no atlas is available.

4 Conclusion

A topological based clustering method has been proposed for the segmentation of the cortex in fetal brain MR images, which takes advantages of anatomical knowledge. The validation performed on T2-weighted images illustrates the usefulness of such structural constraints in an atlas-free approach of fetal brain segmentation.

Further work will focus on the improvement of the segmentation method, such as a better integration of the regularization step into the process, its validation on additional cases and the segmentation of other tissues and structures of the fetal brain.

References

1. M. Bach Cuedra, M. Schaer, A. André, L. Guibaud, S. Eliez, and J.-Ph. Thiran. Brain tissue segmentation of fetal MR images. In *Image Analysis for the Developing Brain, Workshop in MICCAI*, 2009.
2. A. Buades, B. Coll, and J. M. Morel. A review of image denoising algorithms, with a new one. *Multiscale Modeling & Simulation*, 4:490–530, 2005.
3. B. Caldairou, N. Passat, P.A. Habas, C. Studholme, and F. Rousseau. A non-local fuzzy segmentation method: Application to brain MRI. *Pattern Recognition*, in press, doi: 10.1016/j.patcog.2010.06.006.
4. I. Claude, J.-L. Daire, and G. Sebag. Fetal brain MRI, segmentation and biometric analysis of the posterior fossa. *IEEE Transactions on Biomedical Engineering*, 51:617–626, 2004.
5. A. Gholipour, J. Estroff, C. Barnewolt, S. Connolly, and S. Warfield. Fetal brain volumetry through MRI volumetric reconstruction and segmentation. *International Journal of Computer Assisted Radiology and Surgery*, in press, doi: 10.1007/s11548-010-0512-x.
6. P.A. Habas, K. Kim, D. Chandramohan, F. Rousseau, O.A. Glenn, and C. Studholme. Statistical model of laminar structure for atlas-based segmentation of the fetal brain from in-utero MR images. In *SPIE*, volume 7259, pages 17–24, 2009.
7. P.A. Habas, K. Kim, F. Rousseau, O.A. Glenn, A.J. Barkovich, and C. Studholme. Atlas-based segmentation of developing tissues in the human brain with quantitative validation in young fetuses. *Human Brain Mapping*, 31:1348–1358, 2010.
8. K. Kim, P.A. Habas, F. Rousseau, O.A. Glenn, A.J. Barkovich, and C. Studholme. Intersection based motion correction of multislice MRI for 3-D in utero fetal brain image formation. *Medical Imaging, IEEE Transactions on*, 29:146–158, 2010.
9. M. Murgasova, L. Dyet, D. Edwards, M. Rutherford, J. Hajnal, and D. Rueckert. Segmentation of brain MRI in young children. *Academic Radiology*, 14:1350–1366, 2007.
10. L. Najman and H. Talbot. *Mathematical morphology: from theory to applications*. ISTE / J. Wiley & Sons, 2010.
11. L. Perkins, E. Hughes, L. Srinivasan, J. Allsop, A. Glover, S. Kumar, N. Fisk, and M. Rutherford. Exploring cortical subplate evolution using magnetic resonance imaging of the fetal brain. *Developmental Neuroscience*, 30:211–220, 2008.
12. D.L. Pham, P.-L. Bazin, and J.L. Prince. Digital topology in brain imaging. *Signal Processing Magazine, IEEE*, 27:51–59, 2010.
13. M. Prastawa, J.H. Gilmore, W. Lin, and G. Gerig. Automatic segmentation of MR images of the developing newborn brain. *Medical Image Analysis*, 9:457–466, 2005.
14. F. Rousseau, O. Glenn, B. Iordanova, C. Rodriguez-Carranza, D. Vigneron, J. Barkovich, and C. Studholme. Registration-based approach for reconstruction of high-resolution in utero fetal MR brain images. *Academic Radiology*, 13:1072–1081, 2006.
15. M. Rutherford, S. Jiang, J. Allsop, L. Perkins, L. Srinivasan, T. Hayat, S. Kumar, and J. Hajnal. MR imaging methods for assessing fetal brain development. *Developmental Neurobiology*, 68:700–711, 2008.
16. H. Xue, L. Srinivasan, S. Jiang, M. Rutherford, A.D. Edwards, D. Rueckert, and J.V. Hajnal. Automatic segmentation and reconstruction of the cortex from neonatal MRI. *NeuroImage*, 38:461–477, 2007.